Acta Neuropathol (2005) 109: 643–653
DOI 10.1007/s00401-005-1007-7

CASE REPORT

**Judit Miklossy · Ian R. Mackenzie
Katerina Dorovini-Zis · Donald B. Calne
Zbigniew K. Wszolek · Andis Klegeris
Patrick L. McGeer**

Severe vascular disturbance in a case of familial brain calcinosis

Received: 16 February 2005 / Revised: 19 April 2005 / Accepted: 19 April 2005 / Published online: 4 June 2005

Abstract Here we present the first neuropathological study of a case of autosomal dominant brain calcinosis in a family followed through five generations. The 71-year-old female who came to autopsy had unusually severe and extensive bilateral brain calcifications. The process appeared to start with deposition of minute calcium-positive spheroids of less than 1 μm in diameter in capillaries that otherwise appeared normal. These could be observed extending to areas distant from the main pathology. In more advanced stages, larger spheroids completely covered some capillaries while sparing others. In heavily affected regions, ghost capillaries were observed where only calcium spheroids remained after endothelial cells and basement membranes had disappeared. Vessels of all sizes were affected, and large accretions were observed in the basal ganglia, thalamus and cerebellum. Combined scanning electron microscopy and X-ray spectrometry of these large deposits revealed a dominant presence of calcium and phosphorous, plus carbon and oxygen indicative of organic material, and small amounts of sodium, potassium, sulfur, and magnesium. Reactive astrocytes and reactive microglia accumulated around the calcified deposits, indicating a mild ongoing inflammatory process. The results suggest that severe vascular impairment and mild inflammation contribute to the slow but inexorable progression of hereditary brain calcinosis.

Keywords Capillaries · Dystonia · Fahr's disease · Gallyas staining · Inflammation

J. Miklossy · A. Klegeris · P. L. McGeer (✉)
Kinsmen Laboratory of Neurological Research,
University of British Columbia, 2255 Wesbrook Mall,
Vancouver, British Columbia, V6T1Z3, Canada
E-mail: mcgeerpl@interchange.ubc.ca
Tel.: +1-604-822-7377
Fax: +1-604-822-7086

I. R. Mackenzie · K. Dorovini-Zis
Department of Pathology, Vancouver General Hospital,
Vancouver, British Columbia, Canada

D. B. Calne
Department of Neurology, University of British Columbia,
Vancouver, British Columbia, Canada

Z. K. Wszolek
Department of Neurology, Mayo Clinic,
Jacksonville, Florida, USA

Introduction

Fahr originally described a condition which later became known as idiopathic basal ganglia calcification (IBGC) [11]. The Fahr's triad, or Fahr's syndrome, included bilateral calcification of the basal ganglia, neuropsychiatric manifestations and hypoparathyroidism. It is now evident that brain calcification typically extends far beyond the basal ganglia. Accordingly, we prefer the term idiopathic brain calcinosis (IBC) rather than IBGC to describe the syndrome. Other terms that have been used include striato-pallido-dentate calcifications (SPDC), bilateral striopallidodentate calcinosis (BSPDC), and cerebrovascular ferrocalcinosis (recently reviewed in [3]).

Calcification of the brain may occur in several pathological conditions, including a variety of infectious, metabolic, and genetic syndromes, or even following radiotherapy [15, 19]. The etiology and pathophysiology of most forms of IBC are unknown. The occurrence of hypoparathyroidism or the absence of parathyroid glands in IBC is well known [4, 8, 15], but IBC cases without parathyroid disturbances are more frequent.

IBC may be sporadic or familial. The familial form is frequently autosomal dominant [3, 25], but IBC with recessive inheritance also occurs. A genetic locus (IBGC1) on chromosome 14q has been demonstrated in one autosomal dominant family [13], but the absence of such a linkage in five other affected families indicates genetic heterogeneity [7, 29].

Here we describe the first neuropathological confirmation of one member of a family with autosomal dominant IBC where the 14q IBGC locus [7] has been ruled

out. The family has been followed for five generations [23]. The unusually extensive brain calcification enabled a detailed analysis of the vascular network and the accompanying pathological deposits to be carried out.

Clinical history

This 71 year old female (III/9 in [23]) had dysarthria and involuntary movements of the lips, jaw, tongue, and mouth commencing at age 10. At age 18, she developed athetoid movements of the right arm, and 10 years later involuntary movements of the left leg followed by those of the right limbs. By age 50, she had a marked dysarthria and an increased tone in all four limbs, especially in the wrists. There was dystonic posturing of both hands. Psychometric testing at that time revealed an IQ of 78 on the WAIS [23]. An initial CT scan, performed at age 52, showed bilateral symmetric calcifications in the basal ganglia, thalamus, and cerebellum and in the subcortical white matter of the occipital, temporal, parietal and frontal lobes. Calcifications were also observed in the frontal and parietal cortex [23]. A second CT scan, performed at age 67, showed similar findings without evidence of progression (Fig. 1). Calcium and copper metabolism was normal, as were the serum levels of calcium, phosphate, and iron.

During her final 20 years she developed generalized dystonia with predominant involvement of the upper half of the body. She had severe dysarthria, dysphagia and periods of depression. In her last physical examination 5 months prior to death, her physician reported that she was mentally intact. There were no pyramidal signs. Her pupils were equal and reactive to light, and accommodation and external ocular movements were intact. The patient experienced repeated falls during her last 7 months. Terminally, she had several transient ischemic attacks and episodes of aspiration pneumonia secondary to progressive dysphagia. She died from a radiologically confirmed aspiration pneumonia. Three affected sons of the patient are still alive (pedigrees IV 24, 26, 28; [23]).

Neuropathological investigation

The autopsy, which was restricted to brain, was performed following a postmortem delay of 8 h. One hemisphere of the brain was directly fixed in 10% formalin, and the other dissected in the fresh state with some parts being frozen and others fixed in buffered 4% paraformaldehyde. Blocks were taken from both hemispheres from the middle frontal, frontobasal, middle temporal, primary motor, parietal and occipital cortices; hippocampus; insula; basal ganglia; thalamus; mesencephalon; pons; medulla oblongata; cervical spinal cord; cerebellum and choroid plexus. The formaldehyde-fixed blocks were embedded in paraffin by standard techniques. Sections, 3–5 μm thick, were then cut for detailed analysis. From the paraformaldehyde-fixed blocks, 30- to 100-μm-thick sections were cut on a freezing microtome. These were mostly stained as free-floating sections. Sections from all blocks were subjected to routine cresyl violet and hematoxylin and eosin analysis.

The antibodies used for imunohistochemistry are shown in Table 1 along with the dilutions employed. For detection of antibody binding, the avidin-biotin-peroxidase technique was employed, using a final reaction solution containing 3, 3'-diaminobezidine (DAB, Sigma, D5637) alone to produce a brown reaction product, or combined with 0.6% nickel ammonium sulfate to produce a dark-purple reaction product as previously described in detail [1]. Assessment for Alzheimer-type pathology was performed as described previously [27].

Analysis of vascular involvement using Gallyas technique and immunohistochemistry

To analyze the involvement of capillaries in calcified areas, 100-μm-thick paraformaldehyde-fixed sections were stained with the Gallyas silver technique for capillaries [12]. To detect endothelial cells and basement

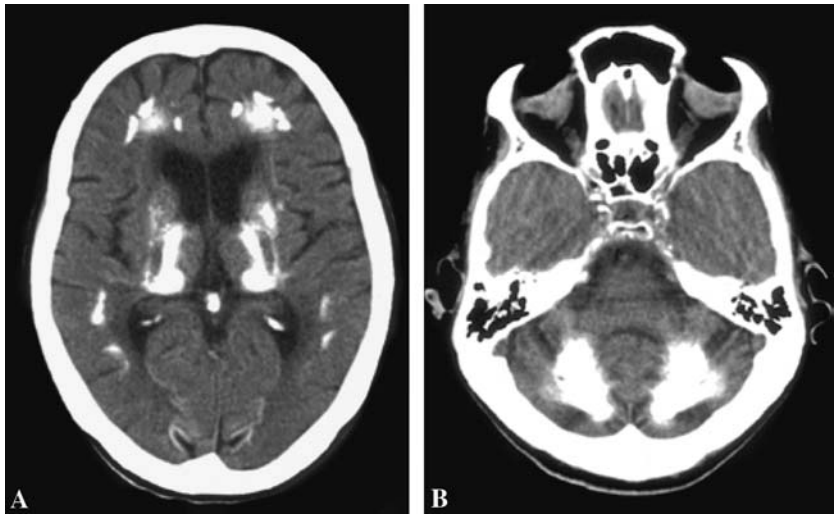

Fig. 1 Extensive bilateral, symmetric calcifications in the brain as revealed by CT scan. **A** Extensive calcifications in the basal ganglia and in the frontal white matter. **B** Massive bilateral cerebellar calcification in the area of the nucleus dentatus

Table 1 Antibodies used in immunohistochemistry

Antigen	Antibody	Source	Type	Dilution
β Amyloid M 0872	Clone 6F/3D	DakoCytomation, Carpinteria, CA	Mouse IgG	1:1,000
cowGFA -GFAP	Z 0334	"	Rabbit IgG	1:5,000
Tau, C-243–441	A0024	"	Rabbit IgG	1:1,000
Ubiquitin	Z 0458	"	Rabbit IgG	1:1,000
LFA-1α (CD11a)	MHM24 (7)	"	Mouse IgG	1:1,000
LCA	M 0701	"	Mouse IgG	1:1,000
Fibrinogen	A0080	"	Rabbit IgG	1:500
Factor VIII	A 0082	"	Rabbit IgG	1:1,000
HLA-DR CR3/43	M 0775	"	Mouse IgG	1:2,000
MBP, MCA 868	Clone 22	Serotec, Oxford, UK	Rabbit IgG	1:1,000
α-Synuclein	Clonelb509	Zymed Lab, San Francisco, CA	Mouse IgG1	1:1,000
α-Synuclein	VP-A106	Vector Labs, Burlingame, CA	Mouse IgG	1:1,000
Anti-neurofilament	010020	Bio-Science, Emmenbruecke, Switzerland	Mouse ascites	1:1,000
Collagen IV	1340–01	Southern Biotech Assoc., Birmingham, AL	Goat IgG	1:1,000
ICAM-1, C2969	8.4A6, D2	Sigma-Aldrich, St. Louis, MO	Mouse, IgG,	1:1,000

membranes, 30-μm-thick sections were immunostained for Factor VIII and collagen type IV, respectively.

Immunohistochemical analysis of inflammation

To analyze whether chronic inflammation accompanies calcification, sections from all brain areas were immunostained with HLA-DR and glial fibrillary acidic protein (GFAP) antibodies to detect reactive microglia and astrocytes, respectively. As markers of ongoing inflammation, antibodies to intercellular adhesion molecule-1 (ICAM-1, CD54) and its ligand the lymphocyte function-associated antigen 1 (LFA-1, CD11a) were employed.

Analysis of the blood-brain barrier

The permeability of the blood-brain barrier was assessed by immunostaining 3-μm-thick paraffin sections from selected regions of the cerebral hemispheres and striatum with an antibody to fibrinogen, a 340,000 molecular weight plasma protein. For immunostaining 3-amino-9-ethylcarbazole (AEC) was used as chromogen producing a red end product and the sections were counterstained with hematoxylin.

Analysis of the calcification using scanning electron microscopy equipped with energy-dispersive X-ray spectrometer

A calcified mass of roughly 1-cm diameter was detached from the cerebellar white matter along with a somewhat smaller sample from a non-calcified area of the occipital cortex. The samples were dried on a hot plate at 40°C for 2 days and were then analyzed by scanning electron microscopy (SEM) at 20 Pa pressure. The energy-dispersive X-ray spectrometer (EDX) detected the X-rays given off by the sample when exposed to a 20-kV electron beam. Images were taken with a backscattered detector. To remove any organic material, a second SEM-EDX analysis of the cerebellar sample was performed following NaOH treatment. A 50-mg sample of the calcified tissue was incubated in 500 μl 2 N NaOH for 30 min at room temperature, then boiled for 5 min. Following centrifugation at 10,000 rpm for 15 min, the pellet was dried overnight in a vacuum desiccator and then analyzed with SEM-EDX.

Primary brain endothelial and astrocytic culture

Brain microvessel endothelial cells and astrocytes were isolated and cultured as previously described [9, 16]. Confluent cultures of endothelial cells and astrocytes were stained with the von Kossa technique for the demonstration of calcium.

Results

Neuropathological findings

The large cerebral arteries did not show atherosclerosis, there was no cortical atrophy and only a moderate dilatation of the lateral ventricles was seen. In coronal slices, extensive whitish-yellow granular lesions were observed in the basal ganglia, thalamus and in the central white matter of cerebellum. Solid calculi with irregular surfaces were observed in these latter two areas. Their size varied from a few millimeters to more than one centimeter in diameter. Similar, but finely granular calcifications were observed in the deep white matter of the frontal, temporal and parietal lobes. In several cortical areas at the depths of some sulci, linear, brownish discolorations were observed. Similar discoloration was also seen in the tegmentum of the brainstem. The substantia nigra and locus ceruleus appeared normal.

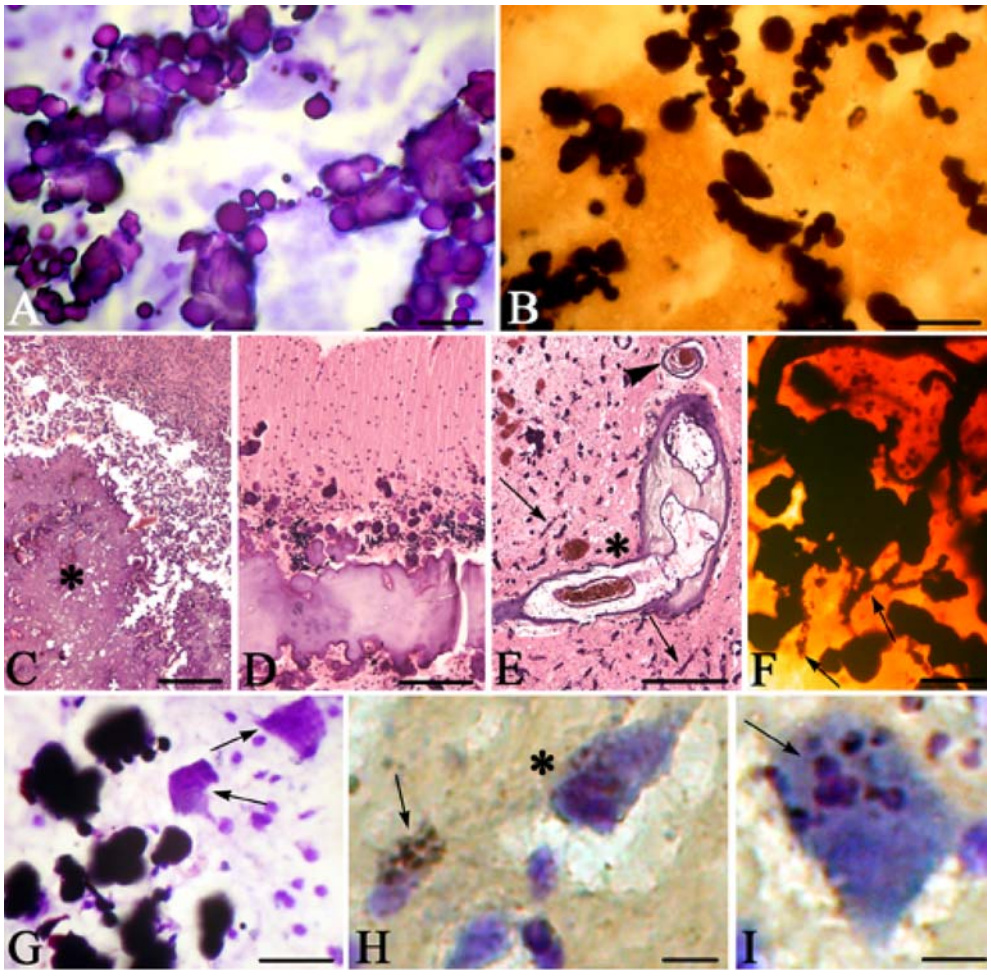

Fig. 2 Calcifications of the brain and brain blood vessels. **A** Extensive calcification in the deep temporal white matter. Cresyl violet. **B** Calcification in the basal ganglia. The von Kossa silver impregnation technique shows the calcium component (*black*) of the pathological deposits. **C** HE staining showing severe calcification in the thalamus. **D** HE staining showing laminar calcification occupying the granular layer of the cerebellum. **E** HE staining of a section of the basal ganglia. Large (*asterisk*), medium-sized (*arrowhead*) and small (*arrows*) vessels all show calcification. **F** The Gallyas silver technique for visualization of cerebral blood vessels showing large calcifications of varying size and shape in the deep white matter of the temporal cortex related to calcified blood vessels (*arrows*). **G** Cresyl violet staining of the basal ganglia. Note the good preservation of nerve cells (*arrows*) around calcium deposits. **H** von Kossa-positive dark intracytoplasmic granules in the cytoplasm of a neuron (*asterisk*) and in a glial cell (*arrow*). Double staining with von Kossa and cresyl violet. **I** Calcified area of the occipital cortex. High-power magnification of von Kossa-positive intracytoplasmic granules in a neuron (*HE* hematoxylin and eosin). *Bars* **A** (also for **B**) 120 μm; **C** 600 μm; **D**, **E** 500 μm; **F** 150 μm; **G** 80 μm; **H** 30 μm; **I** 20 μm

Microscopic examination confirmed the presence of extensive brain calcifications (Fig. 2A–F). The deposits showed a black reaction for calcium by the von Kossa technique (Fig. 2B). The calcifications were in the form of spherical, oval, or elongated cylindrical structures of varying size. They occurred along blood vessels but the larger deposits were apparently free in the neuropil (Fig. 2D). Diffuse, severe calcifications were present in the deep white matter of the frontal, parietal and temporal lobes (Fig. 2A). The pallidum and large parts of the putamen showed extensive calcifications. In the thalamus and cerebellum there were large solid concretions (Fig. 2C, D). Calcifications confined to the cerebral cortex were present in the frontal, parietal and occipital areas. The distribution of the cortical calcifications was pseudolaminar, affecting the deep cortical layers, and mostly localized to sulcal depths. The primary visual cortex was particularly affected. In the brainstem, the calcifications were more extensive in the tegmentum of the medulla.

Calcifications of arteries and veins (Fig. 2E) were observed in addition to capillaries (Fig. 2F). Some large arteries and veins showed complete calcification of their walls, while in other arteries the calcification was restricted to the media. In heavily calcified areas the majority of blood vessels were covered by numerous small calcium spheroids (Fig. 2F).

In calcified gray matter areas, a high number of surviving neurons was seen (Fig. 2G–I). On sections double-stained with von Kossa and cresyl violet, von Kossa-positive intracytoplasmic granules were observed in some neurons and astrocytes (Fig. 2H, I).

Some β amyloid deposits in all cortical areas and in the walls of some leptomeningeal and cortical vessels

and a moderate number of neurofibrillary tangles were seen in the entorhinal cortex, and rarely in the insular cortex and substantia nigra.

Analysis of vascular involvement using Gallyas technique and immunohistochemistry

Use of the Gallyas silver impregnation technique for cerebral vessels [12] enabled us to analyze in detail some aspects of the vascular pathology. With short times of silver impregnation, only calcified structures were stained in areas of cortical involvement. These were composed of innumerable 3- to 10-μm-diameter spheroids arranged in an ordered way, tracing capillary pathways (Fig. 3A, C). With longer impregnation times, when both the calcifications and the capillary network were stained (Fig. 3B, D), it became evident that segments of calcified and spared capillaries were alternated in a random distribution (Fig. 3D). Thin 1- to 2-μm filaments connecting calcified capillaries were frequently present in these areas (Fig. 3E, F). At high magnification, minute calcified spheres were seen attached to the surface of vessel walls (Fig. 3G, H). In addition to the typical 3- to 10-μm spherules covering capillaries, some smaller than 1 μm were also seen (Fig. 3H). Some large cortical blood vessels showed irregularity of their wall (Fig. 3I), were tortuous (Fig. 3J), and sometimes formed loops (Fig. 3K). Peculiar, focalized, fusiform dilatations were frequently observed at the branching areas of blood vessels (Fig. 3L).

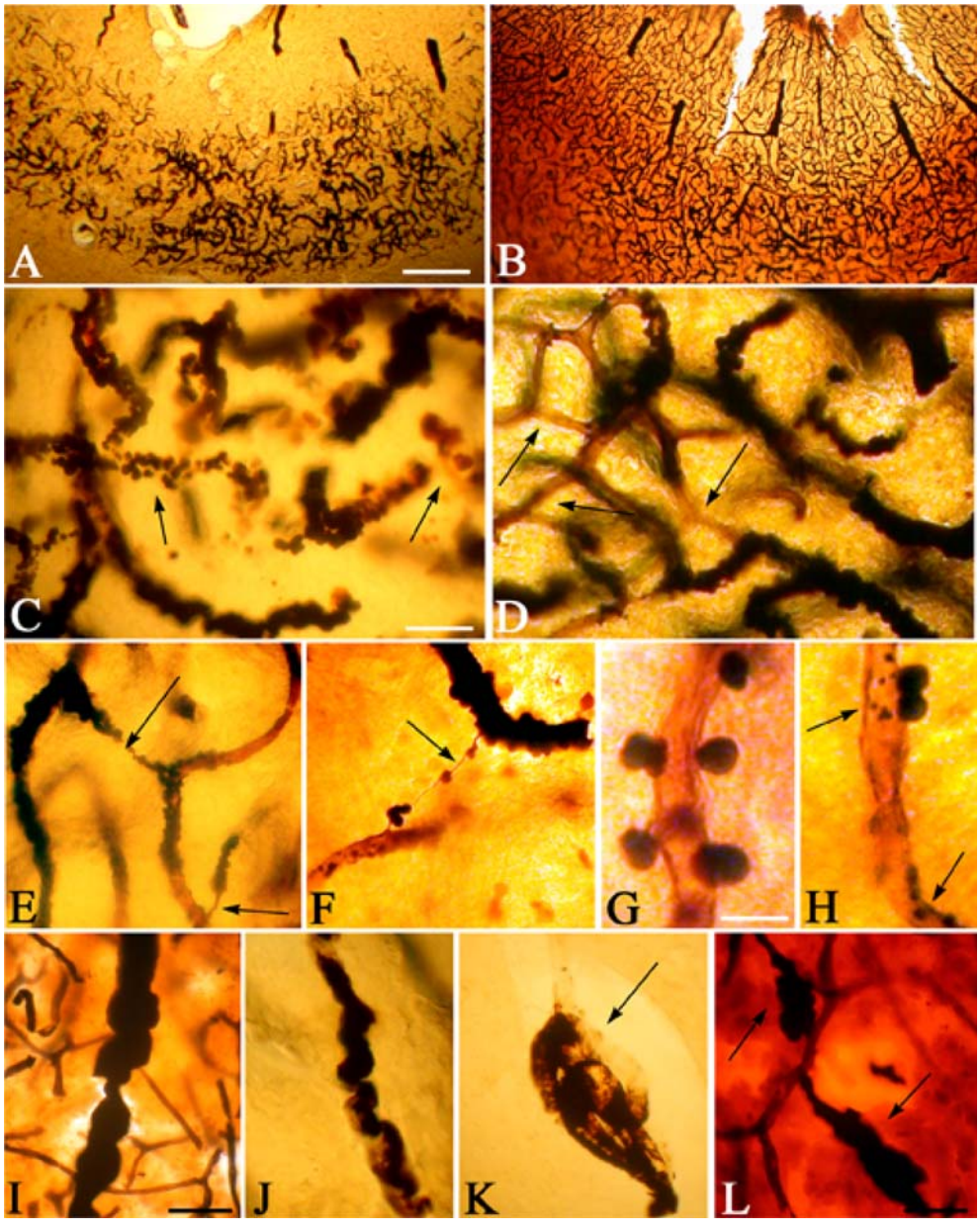

Fig. 3 Calcifications of occipital cortex blood vessels as shown by the Gallyas silver technique. **A** Weak staining impregnates only the calcified deposits, which occur in deeper layers. **B** Stronger silver impregnation reveals the complete capillary network in all cortical layers. The calcium deposits alone (**A**, **C**) highlight an irregular pattern along capillaries. They have a pseudolaminar distribution in deep cortical layers and are preferentially located in sulcal depths. At higher magnification (**C**), the rows of individual fine spherules of calcium deposits are clearly visible. On sections where both the calcium deposits and capillaries are stained (**D**), it is clearly seen that the calcification of the capillary network is partial. **E**, **F** Thin filaments connecting calcified capillaries (*arrows*). **G** Individual calcium spherules attached to the outer surface of a capillary. **H** In addition to large calcium spheroids, small (even less than 1 μm) are also present. **I**–**L** Irregular (**I**) and tortuous (**J**) cortical vessels, sometimes forming loops (**K**, *arrow*) in the cerebral cortex of the insula. Focal, fusiform dilatations (**L**) at branching sites of blood vessels. Temporal cortex. *Bars* **A** (also for **B**) 1 mm; **C** (also for **D**–**F**) 30 μm; **G** alsofor **H**) 12 μm; **I** (also for **J**, **K**) 60 μm; **L** 50 μm

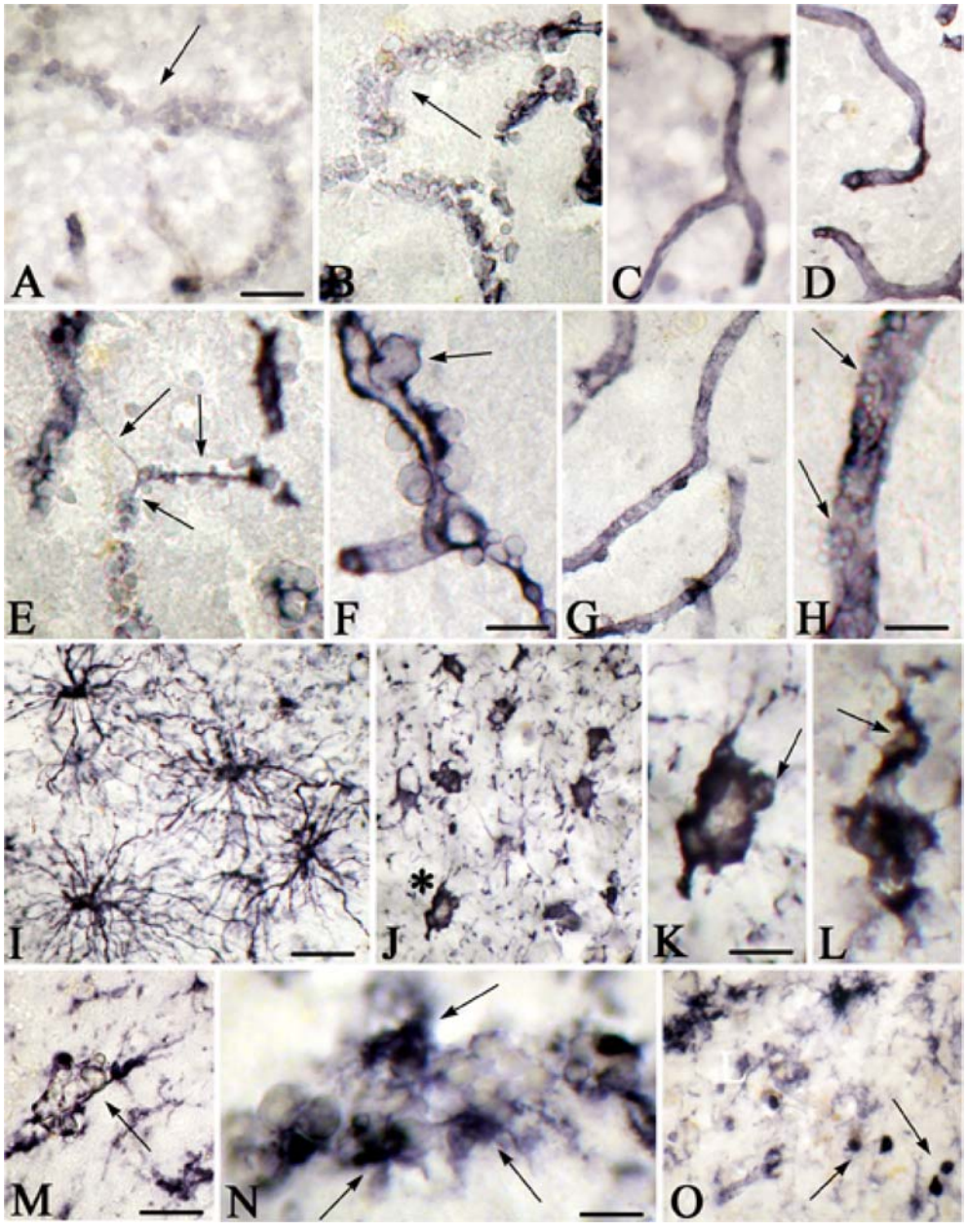

In severely involved capillaries, there was no visible immunostaining for Factor VIII (Fig. 4A) or collagen type IV (Fig. 4B) along the calcium tracks, suggesting that the endothelial cells had died and the basement membrane absorbed. In spared cortical areas, however, normal capillaries demonstrated typical immunostaining for Factor VIII (Fig. 4C) and collagen type IV (Fig. 4D). Thin collagen type IV-positive filaments in the absence of endothelial cells were also frequently seen in calcified areas (Fig. 4E), suggesting that endothelial cells disappear before the collagen type IV basement membrane. In some severely calcified blood vessels, the distribution of collagen type IV was thickened and irregular, sometimes covering calcified spheres on the outer surface of the vessel wall (Fig. 4F). Despite the normal appearance of some capillaries when immunostained with collagen type IV (Fig. 4G), at high magnification they displayed many minute (1 μm or less) calcium deposits (Fig. 4H) indicative of very early stages of calcification.

Immunohistochemical detection of chronic inflammation

Reactive astrocytes immunopositive for ICAM-1 and GFAP (Fig. 4I–L) and reactive microglia immunopositive for HLA-DR and LFA-1 (Fig. 4M, N) were observed around severe brain calcifications. Astrocytes in subcortical areas demonstrated typical reactive mor-

◀

Fig. 4 **A**–**H** Involvement of the walls of calcified vessels in the occipital cortex. **A**, **B** Calcified capillaries show negative reactivity to Factor VIII (**A**) and collagen type IV (**B**) (*arrows*). Compare the decreased immunoreactivity of these calcified capillaries with those analyzed in a spared cortical area (**C** Factor VIII; **D** collagen type IV). **E** Thin, collagen type IV positive filaments (*arrows*) connecting calcified capillaries. **F** An irregular pattern of collagen type IV is visible, sometimes covering calcium spheroids (*arrow*). **G** At the periphery of cortical calcifications, on apparently spared capillaries immunostained for collagen type IV, at high magnification innumerable minute calcium deposits are present along the capillary (**H**). **I**–**O** Presence of chronic inflammation. **I** ICAM-1-positive reactive astrocyes in the subcortical area of the temporal cortex with radially arranged long processes. **J** ICAM-1-positive reactive astrocytes with an unusual appearance in the vicinity of calcium deposits in the basal ganglia. They show intracytoplasmic whitish-yellow granules. **K** Higher magnification of the asterisk area in **J**. **L** Reactive astrocyte, showing similar morphology in the same area as **J** and **K**, immunostained with GFAP. **M**, **N** Clumps of reactive microglia (*arrows*) overexpressing LFA-1, closely surrounding calcium deposits in the basal ganglia. **O** Increased numbers of reactive microglia accompanied by LFA-1-positive round cells (*arrows*) compatible with activated T cells. *Bars* **A** (also for **B**–**E**, **G**) 30 μm; **H** 10 μm; **F** 30 μm; **I** (also for **J**) 80 μm; **K** (also for **L**) 30 μm; **M** (also for **O**) 100 μm; **N** 50 μm

phology with numerous radial processes (Fig. 4I). However, in areas of calcification, atypical reactive astrocytes with few cell processes had accumulations of fine intracytoplasmic whitish-yellow granules, suggestive of calcium deposits (Fig. 4J–L). In the same affected areas, LFA-1 (CD11a), which is the counter receptor of ICAM-1, was overexpressed in clumps of reactive microglial cells closely associated with pathological calcium deposits (Fig. 4M, N). Slightly increased numbers of LFA-1-positive and leukocyte common antigen (LCA)-positive round cells, morphologically compatible with lymphocytes, were also present in these areas (Fig. 4O).

Analysis of the blood-brain barrier

In the spared gray and white matter, fibrinogen was detected only within the lumen of normal blood vessels (Fig. 5A). In areas of calcification, the perivascular tissue stained diffusely positive for fibrinogen (Fig. 5B). In a small number of microvessels, fibrinogen-positive, small globular bodies were deposited in and around the wall of the involved vessels (Fig. 5C). In areas of fibrinogen leakage, the bodies and processes of reactive astrocytes showed intense staining for fibrinogen (Figs. 5B, D). Within the surrounding intact tissue, occasional spared vessels were associated with perivascular diffusion of fibrinogen (Fig. 5E). Perivascular cells and scattered microglial cells in areas of calcification showed strong expression of class II MHC molecules (Fig. 5F).

SEM equipped with EDX spectrometry

The results of the SEM-EDX analysis of a large cerebellar calcium deposit are illustrated in Fig. 6. The SEM revealed that the pathological deposits consisted of bright and dark areas. X-ray spectrometry showed that the composition of bright and dark areas was qualitatively similar, demonstrating a major presence of calcium, phosphorus, carbon and oxygen, plus detectable amounts of sodium, sulphur, potassium, and magnesium. However, the bright areas showed high concentrations of calcium and phosphorus, indicative of calcium phosphate, and the dark areas high concentrations of carbon and oxygen, suggesting the incorporation of organic material. Following NaOH treatment, the dark areas disappeared and the remaining material was enriched in calcium and phosphorous comparable to the untreated bright areas. There was no difference in the composition between the calcified material of the cerebellar white matter and that of the occipital cortex.

Primary brain endothelial and astrocytic culture

Primary cultures of endothelial cells exhibited a normal growth pattern and formed typical contact-inhibiting monolayers. There was no evidence of abnormal cytoplasmic or extracellular deposition of calcium after 12 days in culture in endothelial cells and after 3 weeks in culture in astrocytes.

Discussion

The main neuropathological finding of this 71-year-old mother of three affected sons consisted of an unusually severe and extensive calcification of highly selective areas of the brain. The distribution closely followed the pattern described in Fahr's disease [11]. In our case, the dorsomedial nucleus of the thalamus was also strongly affected. The clinical observations of diffuse, generalized dystonia combined with progressive pseudobulbar palsy and dysphagia is in good correlation with the observed calcifications of the basal ganglia, thalamus and brainstem tegmentum. The combined use of SEM and EDX showed that the main components of the bright areas of calcification consisted of calcium phosphate, with oxygen, carbon, potassium, sodium, magnesium, and sulfur also being identified. Iron levels were below the detection limit of 0.2% by weight. A few reports, using laser spectrographic analysis of some IBC cases, have demonstrated the presence of aluminum and iron in addition to the elements identified in our case [10, 20, 21, 30]. This may relate to the sensitivity of the technique being used. In agreement with previous IBC reports [30], no difference in the elementary composition was found between different calcified areas.

The use of the Gallyas silver technique [12] showed that the calcification of blood vessels was partial. On Gallyas-silver impregnated as well as collagen type IV-immunoreactive capillaries, mature calcified spheres were detected budding from, and attached to, the outer surface of vessel walls, while tiny, perhaps immature

spheres, were detected on apparently spared capillaries at the periphery and even at a considerable distance around calcified areas. The decrease or absence of Factor VIII and collagen type IV in some calcified capillary tracks indicates that the calcification process eventually causes degeneration, leading to ghost capillaries. The presence of collagen type IV-positive and Factor VIII-negative filaments indicates that the demise commences with death of endothelial cells with ground substance remaining, although both eventually disappear. Previous SPECT studies have shown bilaterally reduced cerebral perfusion in calcified basal ganglia; indicating a direct relationship between this vascular disturbance and dystonic symptoms [32]. The neuronal loss we observed in gray matter areas with extensive calcification is also consistent with these observations.

In the vicinity of calcified areas, astrocytes with peculiar morphology showed intracytoplasmic accumulations of a fine whitish-yellow granular material. The granules, which were sometimes van Kossa positive, may represent internalized calcified material. Previous ultrastructural studies showed that in IBC calcified material can be internalized by macrophages and astrocytes [14].

Analysis of the blood-brain barrier showed that extravasation and perivascular deposition of fibrinogen was focally associated with areas of calcification, indicating increased permeability of the abnormal vessels similarly to the focal blood-brain barrier abnormalities reported in long-standing lesions in multiple sclerosis [22]. The occasional presence of fibrinogen-positive globules in association with calcified microvessels suggests that plasma proteins that pass through the disrupted blood-brain barrier may sequester in these areas and form the nidus for mineral deposition. The positive staining of perivascular astrocytes indicates uptake of extravasated fibrinogen, which is similar to that observed following experimental disruption of the blood-brain barrier [5, 18].

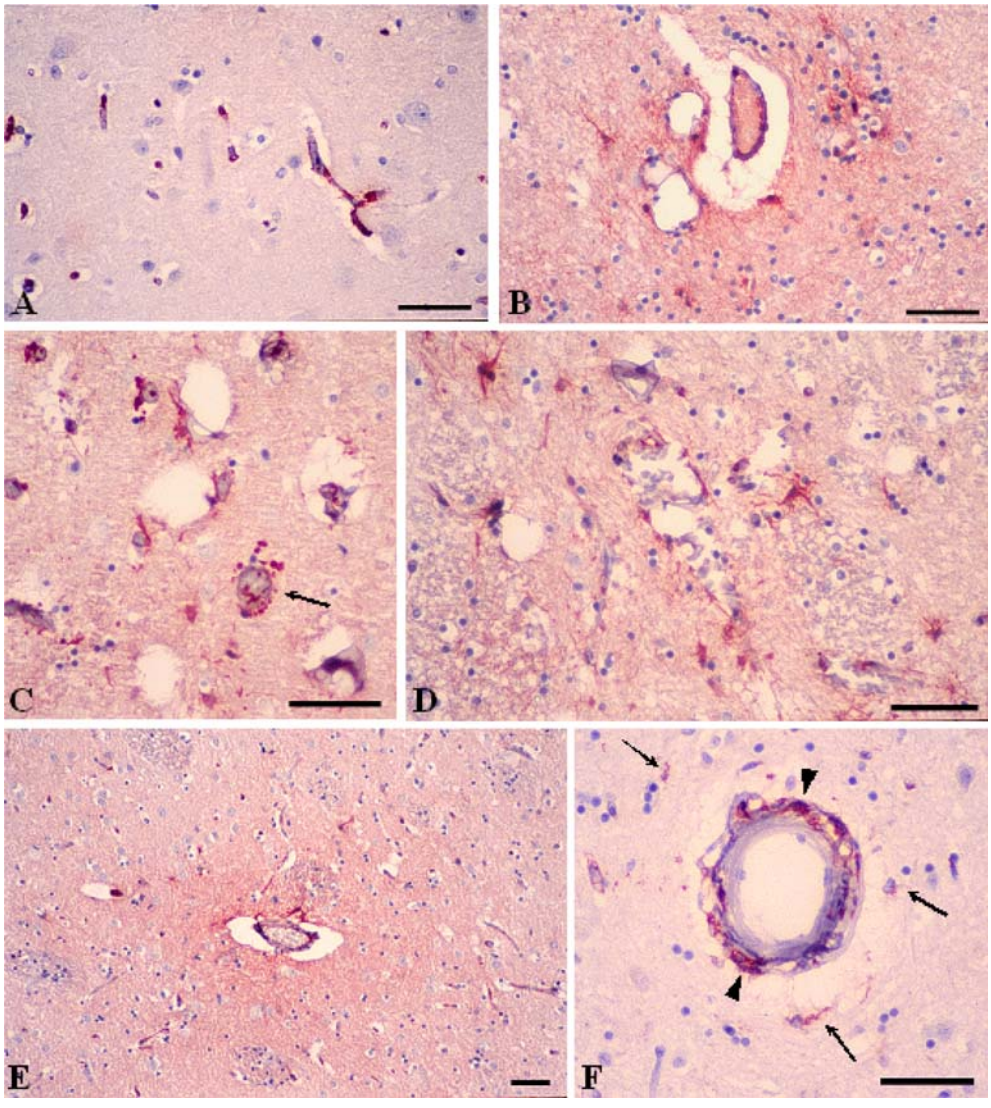

Fig. 5 Increased permeability of the blood-brain barrier in calcified brain areas. For the immunohistochemical analysis, AEC was used as the chromogen producing a *red* positive immunoreaction. The immunostained sections were counterstained with hematoxylin. **A**–**F** Immunoperoxidase staining for fibrinogen. **A** Fibrinogen is present only in the lumen of normal cortical microvessels. **B** Diffuse staining of the extravascular tissue is present in areas of vascular calcification in the striatum. **C** Intensely positive globular bodies (e.g. *arrow*) are deposited in and around the vascular wall of a calcified microvessel. **B**, **D** Reactive astrocytes in areas of blood-brain barrier breakdown show strong cytoplasmic staining indicating fibrinogen uptake. **E** Fibrinogen extravasation around blood vessel adjacent to calcified area in the striatum. **F** Perivascular cells (*arrowheads*) and scattered microglia (*arrows*) are CR3/43 positive. *Bars* 50 μm

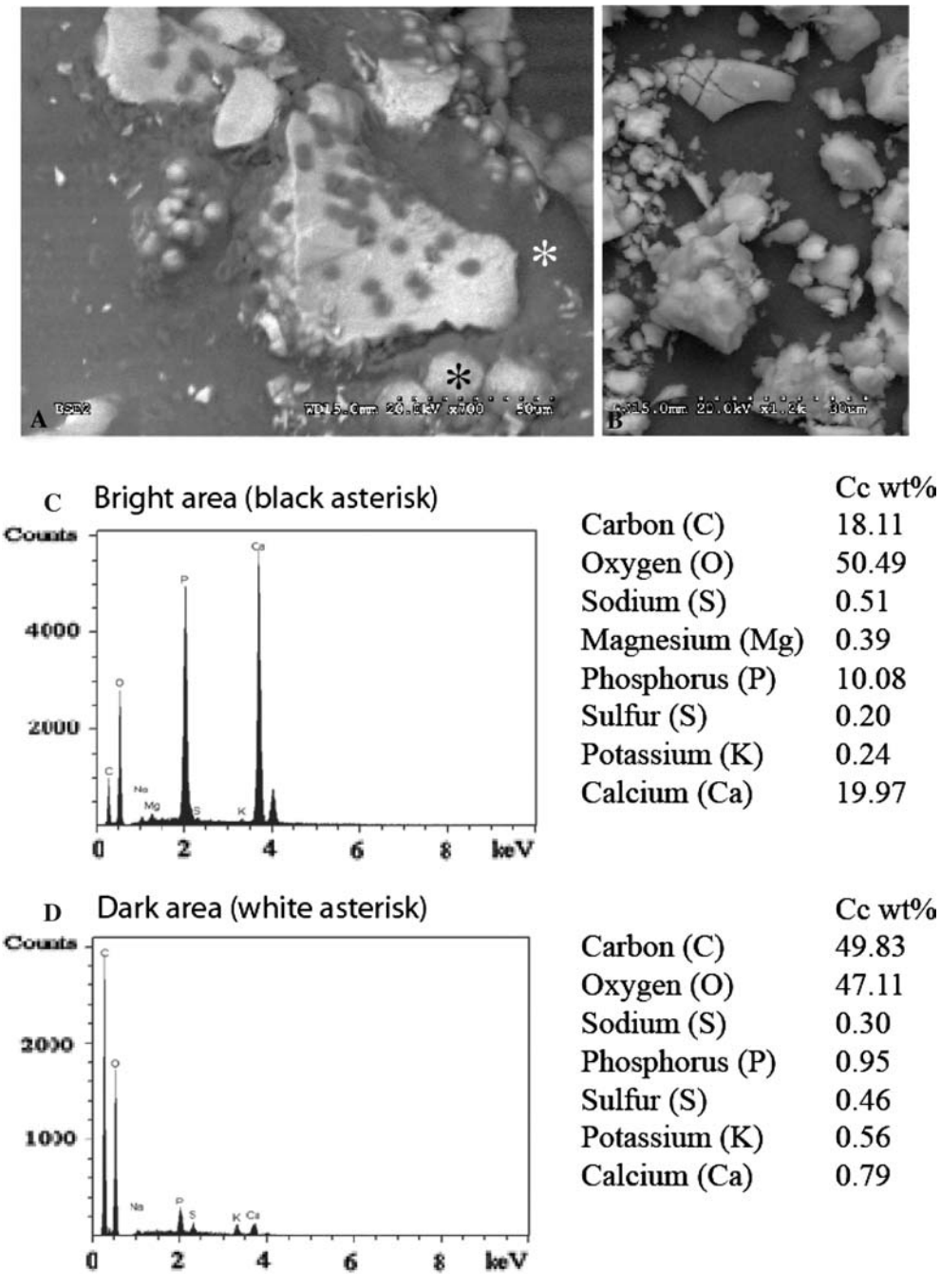

Fig. 6 EDX of a large calcium deposit. **A** The calcified mass consisted of bright (*black asterisk*) and dark areas (*white asterisk*). The bar (*row of dots* at the *right bottom*) corresponds to 50 μm. **B**, **C** EDX spectra obtained by analysis of these bright (**B**) and dark (**C**) areas of the calcified material. Peak locations identify the elements, and the area under the peaks define their concentration in the tissue, expressed in weight percent (wt %). The brighter areas showed a high calcium and phosphorus concentration indicating that the major component is calcium phosphate. The oxygen and carbon concentration and the low calcium and phosphorus content suggest that it corresponds to organic material in the calcified deposit (*EDX* X-ray spectrometry analysis)

It was proposed that a slowly progressive metabolic or inflammatory process, which subsequently causes calcification, may be responsible for the neurological deficit observed in IBC [2]. The role of chronic inflammation in several other neurodegenerative disorders is clearly established [26]. In the brain of our patient, reactive astrocytes overexpressed ICAM-1 and reactive microglia overexpressed LFA-1 around calcified deposits. The presence of these inflammatory molecules and a slightly increased number of LFA-1-positive activated T cells in the affected areas are indicative of an ongoing inflammatory process. The mild degree of inflammation is in harmony with the very slow progression of the disease.

The etiology of IBC remains unknown. It is not clear whether the calcification is secondary to a generalized metabolic disorder associated with the disruption of the blood-brain barrier, or is due to a primary disorder of the central nervous system [13]. The absence of abnormal calcium deposition by primary endothelial cells and astrocytes in vitro suggests that the primary defect in calcium metabolism may not reside in the blood-brain barrier endothelium or in astrocytes.

IBC is frequently associated with various neurodegenerative disorders. A considerable number of IBC cases associated with a slowly progressive atypical presenile dementia, characterized by fronto-temporal atrophy and diffuse neurofibrillary tangle formation, has been reported [17, 28, 31]. In our patient there was no history of dementia and we did not observe diffuse neurofibrillary tangle formation. Parkinsonian symptoms frequently occur in IBGC, but pathological changes in the substantia nigra vary [25]. In our case the substantia nigra did not show Lewy bodies, and there were only minor changes consisting of a few extraneuronal pigment deposits and rare neurofibrillary tangles.

α-Synuclein-immunopositive glial and neuronal cytoplasmic inclusions were described in a case of familial IBC, suggesting that familial IBGC may be a new α-synuclein disorder [25], which was also absent in our patient.

The similarity in clinical manifestations of a case of radiologically diagnosed IBC to corticobasal degeneration was recently reported [33]. The histological analysis excluded corticobasal degeneration in our case. Taken together, these observations suggest that heterogeneity exists not only of the genetic origin, but also of the pathological manifestations of IBC. Further genetic and neuropathological investigations of familial IBC are important as the neuropathological analysis of a representative number of IBC cases may answer the question of whether neurofibrillary tangle formation, Lewy bodies or α-synucleinopathy are age-related associations of IBC, or whether they are associated components of different phenotypes of sporadic or familial IBC. They may help to highlight possible links between the genetic, the clinical, and the pathological manifestations of this peculiar neurodegenerative disorder. The present results show that severe vascular involvement and inflammatory processes may both contribute to the slow progression of the disease.

Acknowledgements We thank Susan Calne, RN for assistance in obtaining the autopsy material. We are grateful to Sheng Yu for help with histology and to Mary Mager for her assistance in the SEM-EDX analysis. This work was supported by grants from the Pacific Parkinson's Research Institute, the Jack Brown and family AD Research Fund as well as donations from individual British Columbians.

References

1. Akiyama H, McGeer PL (1990) Brain microglia constitutively express β-2 integrins. J Neuroimmunol 30:81–93
2. Avrahami E, Cohn DF, Feibel M, Tadmor R (1994) MRI demonstration and CT correlation of the brain in patients with idiopathic intracerebral calcification. J Neurol 241:381–384
3. Baba Y, Broderick DF, Uitti RJ, Hutton ML, Wszolek ZK (2004) Heredofamilial brain calcinosis syndrome. Mayo Clin Proc Rev (in press)
4. Beall SS, Patten BM, Mallette L, Jankovic J (1989) Abnormal systemic metabolism of iron, porphyrin, and calcium in Fahr's syndrome. Ann Neurol 26:569–575
5. Blakemore WF (1969) The fate of escaped plasma protein after thermal necrosis of the rat brain: an electron microscopy study. J Neuropath Exp Neurol 28:139–152
6. Braak H, Braak E, Bohl J (1993) Staging of Alzheimer-related cortical destruction. Eur Neurol 33:403–408
7. Brodaty H, Mitchell P, Luscombe G, Kwok JJ, Badenhop RF, McKenzie R, Schofield PR (2002) Familial idiopathic basal ganglia calcification (Fahr's disease) without neurological, cognitive and psychiatric symptoms is not linked to the IBGC1 locus on chromosome 14q. Hum Genet 110:8–14
8. Delplace PO, Wery D, Lemort M, Baguet J, Jeanmart L (1989) A case of multiple brain calcifications associated with hypoparathyroidism. J Belge Radiol 72:263–266
9. Dorovini-Zis K, Prameya R, Bowman PD (1991) Culture and characterization of microvascular endothelial cells derived from human brain. Lab Invest 64:425–36
10. Duckett S, Galle P, Escourolle R, Poirier J, Hauw JJ (1977) Presence of zinc, aluminum, magnesium in striopallidodentate (SPD) calcifications (Fahr's disease): electron probe study. Acta Neuropathol 38:7–10
11. Fahr T (1930) Idiopathische Verkalkung der Hirngefaesse. Zentralbl Allg Pathol 50:129–133
12. Gallyas F (1971) Silver staining of Alzheimer's neurofibrillary changes by means of physical development. Acta Morphol Acad Sci Hung 19:1–8
13. Geschwind DH, Loginov M, Stern JM (1999) Identification of a locus on chromosome 14q for idiopathic basal ganglia calcification (Fahr disease). Am J Hum Genet 65:764–772
14. Guseo A, Boldizsar F, Gellert M (1975) Electron microscopic study of striatodental calcification (Fahr). Acta Neuropathol (Berl) 31:305–313
15. Harrington MG, Macpherson P, McIntosh WB, Allam BF, Bone I (1981). The significance of the incidental finding of basal ganglia calcification on computed tomography. J Neurol Neurosurg Psychiatry 44:1168–1170
16. Hosokawa M, Klegeris A, McGeer PL (2004) Human oligodendroglial cells express low levels of C1 inhibitor and membrane cofactor protein mRNAs. J Neuroinflammation 24:1–17
17. Ikeda M, Tanabe H, Mori T, Komori K, Nakagawa Y, Tanimukai S, Nishimura T, Ikeda K (1994) A case of atypical presenile dementia. No To Shinkei 46:175–181
18. Klatzo I, Miquel J, Otenasek R (1962) The application of fluorescently labeled serum proteins (FLSP) to the study of vascular permeability in the brain. Acta Neuropathol (Berl) 2:144–160
19. Koller WC, Cochran JW, Klawans HL (1979) Calcification of the basal ganglia: computerized tomography and clinical correlation. Neurology 29:328–333
20. Kozik M, Kulczycki J (1978) Laser-spectrographic analysis of the cation content in Fahr's syndrome. Arch Psychiatr Nervenkr 225:135–142
21. Kuran W, Kozik M, Kulczycki J (1981) Laser-spectroscopic analysis of pseudocalcium deposits in Fahr's syndrome. Neurol Neurochir Pol 15:397–401
22. Kwon EE, Prineas JW (1994) Blood-barrier abnormalities in longstanding multiple sclerosis lesions: an immunohistochemical study. J Neuropathol Exp Neurol 53:625–636
23. Larsen TA, Dunn HG, Jan JE, Calne DB (1985) Dystonia and calcification of the basal ganglia. Neurology 35:533–537
24. Lhatoo SD, Perunovic B, Love S, Houlden H, Campbell MJ (2003) Familial idiopathic brain calcification—a new and familial alpha-synucleinopathy? Eur Neurol 49:223–226
25. Manyam BV, Walters AS, Keller IA, Ghobrial M (2001) Parkinsonism associated with autosomal dominant bilateral striopallidodentate calcinosis. Parkinsonism Relat Disord 7:289–295
26. McGeer PL, McGeer EG (2002) Local neuroinflammation and the progression of Alzheimer's disease. J Neurovirol 8:529–538
27. Miklossy J, Kraftsik R, Pillevuit O, Genton C, Bosman FT (1998) Curly fibers and tangle-like inclusions in the ependyma and choroid plexus—a pathogenetic relationship with the cortical Alzheimer's type changes? J Neuropathol Exp Neurol 57:1202–1212

28. Nomoto N, Sugimoto H, Iguchi H, Kurihara T, Wakata N (2002) A case of Fahr's disease presenting "diffuse neurofibrillary tangles with calcification". Rinsho Shinkeigaku 42:745–749
29. Oliveira JRM, Spiteri E, Sobrido MJ, Hopfer S, Klepper J, Voit T, Gilbert J, Wszolek ZK, Calne DB, Stoessl AJ, Hutton M, Manyam BV, Boller F, Baquero M, Geschwind DH (2004) Genetic heterogeneity in familial idiopathic basal ganglia calcification (Fahr disease). Neurology 63:2165–2167
30. Schmitt J, Dietzmann K, Bossanyi P von (1992) Qualitative studies of Fahr disease. Acta Histochem Suppl 42:319–324
31. Shibayama H, Kobayashi H, Iwase S, Nakagawa M, Marui Y, Kayukawa Y, Iwata H, Takeuchi T (1986) Unusual cases of presenile dementia with Fahr's syndrome. Jpn J Psychiatry Neurol 40:85–100
32. Uygur GA, Liu Y, Hellman RS, Tikofsky RS, Collier BD (1995) Evaluation of regional cerebral blood flow in massive intracerebral calcifications. J Nucl Med 36:610–612
33. Warren JD, Mummery CJ, Al-Din AS, Brown P, Wood NW (2002) Corticobasal degeneration syndrome with basal ganglia calcification: Fahr's disease as a corticobasal look-alike? Mov Disord 17:563–567